Pergamon

Int. J. Heat Mass Transfer. Vol. 39, No. 6, pp. 1223–1234, 1996

0017–9310/96 $15.00 + 0.00

0017–9310(95)00195–6

Conjugate mixed convection in a channel: modified five percent deviation rule

C. Y. CHOI

Department of Agricultural and Biosystems Engineering, The University of Arizona, Tucson, AZ 85721, U.S.A.

and

S. J. KIM

Thermal Engineering Center, IBM Storage Systems, Tucson, AZ 85744, U.S.A.

(*First received* 23 *September* 1994 *and in final form* 26 *May* 1995)

Abstract—Three dimensional conjugate mixed convection in a rectangular channel is numerically investigated. The focus is on the effects of local buoyancy generated by a discrete heat source mounted on a thermally conducting board. Calculations cover $0.126 \leqslant Re \leqslant 1260$, $Gr = 7.8789 \times 10^7$, $1 \leqslant \kappa \leqslant 100$, and $Pr = 0.71$, respectively. Flow fields show active interaction between the buoyancy-induced thermal plume and the approaching external flow in the mixed convection regime where the temperature distribution, heat flux, and heat transfer coefficients all strongly depend on such flow interaction. In addition, the Nusselt number on top of the heat source indicates significant three-dimensional effects. The 'modified 5% deviation rule' is proposed in an effort to define the natural, mixed and forced convection regimes. The proposed rule is especially appropriate for conjugate heat transfer problems in which the thermal conductivity of the board plays an important role in determining the heat transfer mode. A correlation for $\theta_{max}/\kappa^{1/2}$ is sought, and the mixed convection regime is accordingly determined as $1.81 \times 10^{-3} \leqslant Re/Gr^{1/2} < 2.80 \times 10^{-2}$.

1. INTRODUCTION

In recent years, mixed convection heat transfer in a channel has been studied primarily by considering either isothermal or adiabatic boundary conditions along the surface on which heat sources are mounted. Consequently, attention has been focused solely on the flow patterns and convective transport phenomena within the fluid. The importance of the buoyancy effect, however, is also determined by the relative magnitude of certain properties, such as the thermal conductivity of the conducting board. The typical electronic package, for example, involves air cooling of electronic components on a thermally conductive printed circuit board. Therefore, an understanding of coupled conduction and convection is crucial when faced with the task of enhancing the thermal performance of electronic components mounted on the board. In addition, one may encounter three-dimensional mixed convection flows above discrete heat sources on a thermally conducting board in a rectangular channel. In this case, the numerical investigation of mixed convection becomes a formidable task due to the complex governing equations. Consequently, simplified geometries in a two-dimensional channel with either a single or multiple heat sources have been considered by many researchers. Simple configurations are advantageous in that basic physics is sufficient to explain the nature of mixed convection and the numerical solutions are not too complicated to understand and interpret. However, mixed convection due to discrete heat sources cannot be completely understood without consideration of three-dimensional effects in many practical situations.

Many researchers have investigated either mixed convection or conjugate forced convection with discrete heat sources in a two-dimensional channel [1–9], and Choi *et al.* [8, 9] have summarized these investigations. However, there are only a few reports available on two-dimensional conjugate mixed convection heat transfer. Kim *et al.* [10] reported conjugate mixed convection in a two-dimensional channel with rectangular blocks. They demonstrated the importance of buoyancy effects as well as conduction through a printed circuit board. In addition, they showed that over-simplified isothermal or adiabatic boundary conditions might not be appropriate for simulating the cooling of modern electronic devices. Papanicolaou and Jaluria [11, 12] extensively studied two-dimensional conjugate mixed convection from a localized heat source in a cavity with two openings. Oscillatory results were observed beyond the critical value of Gr/Re^2, and the results were initially characterized by a single frequency. As Gr/Re^2 increased further, the oscillations showed irregular patterns which indicated that the flow was approaching the turbulent regime.

A relatively small number of three-dimensional mixed convection studies have been reported in the

NOMENCLATURE

A	top surface area of heat source
Gr	Grashof number, $g\beta q''' H^5/k_f \nu^2$
H	overall channel height [m]
h	heat transfer coefficient [W m^{-2} K]
k	thermal conductivity
L	streamwise total channel length [m]
n	dimensionless normal direction coordinate
$\underline{Nu}$	local Nusselt number, equation (7)
$\overline{Nu}$	average Nusselt number, equation (8)
p	pressure [Pa]
P	dimensionless pressure, $p/\rho u_0^2$
Pr	Prandtl number, ν/α
q'''	volumetric heat generation [W m^{-3}]
Re	Reynolds number $u_0 H/\nu$
S	source term, equation (6)
t	thickness of the heat source
T	temperature [°C]
u, v, w	x- y- and z-direction velocities [m s^{-1}]
U, V, W	x- y- and z-direction dimensionless velocities, equation (1b)
x, y, z	dimensional coordinates [m]
X, Y, Z	x- y- and z-direction dimensionless coordinates, equation (1a).

Greek symbols

β	coefficient of thermal expansion [°C^{-1}]
κ	thermal conductivity ratio, k_s/k_f
μ	dynamic viscosity [kg (m s)$^{-1}$]
ν	kinematic viscosity [m^2 s^{-1}]
θ	dimensionless temperature, equation (1c)
ρ	density of fluid [kg m^{-3}].

Subscripts

f	fluid (air)
h	heat source
o	free stream at inlet
s	solid
t	top
u	upstream
w	wall
max	maximum.

literature even without consideration of conjugate effects. Shaw *et al.* [13] studied mixed convection phenomena with an isothermal heating block in a three-dimensional channel. Their research showed that the Nusselt number, as well as the flow field of a three-dimensional channel, is very different from that of a two-dimensional channel. Incropera and co-workers [14–16] conducted a series of experiments to investigate mixed convection resulting from a forced air or water flow in a horizontal plane duct, and they visualized four flow regimes along the bottom plate—laminar, mixed, transitional, and turbulent regimes. Consequently, significant improvement in heat transfer was found to be due to the buoyancy-driven secondary flow. Recently, Huang and Lin [17] numerically investigated the unsteady and transitional characteristics of mixed convection flows of air in a three-dimensional channel. The evolution of these complicated flows was discussed in detail. Mixed convection in a semicircular duct with an axially non-uniform boundary condition on a flat wall has been numerically studied by Karki *et al.* [18]. The study showed the significant effect of the thermal boundary condition along the curved wall on the secondary flow pattern and, therefore, on the heat flux distribution on the heat transfer surface.

In an effort to elucidate the physics of three-dimensional mixed convection, the present study involving both conduction and convection focuses on the effects of local buoyancy generated by a discrete heat source placed on a thermally conducting board. Therefore, the attendant mixed convection that occurs when flow is induced into the channel by external means is also considered. The resulting temperature and pressure distributions, as well as the Nusselt number and the maximum temperature, are of practical interest. The modified '5% deviation rule' is proposed based on the maximum temperature results in order to identify the mixed convection regime.

2. FORMULATION AND NUMERICAL PROCEDURE

The geometry considered in the present study is a rectangular horizontal channel in which a thermally conducting board is located. A volumetric heat source is flush-mounted to the board as shown in Fig. 1. The total channel height ($H = H_t + H_c + H_b$) is chosen as a characteristic length for the non-dimensionalization of the governing equations. In comparison with H, the important dimensions are $H_t = H_b = 0.425H$, $H_c = 0.15H$, $t = 0.025H$, $W = 2.5H$, $W_h = L_h = 0.5H$, $L_f = H$, $L_u = L_b = 2.5H$, and $L_d = 3.5H$. Therefore, the total length of the channel is $10H$. A pressure-driven external flow is maintained throughout the channel in addition to the buoyancy-induced flow. The side walls (at $z = 0$ and W) are adiabatic, and the temperature of the top and bottom walls as well as the inlet flow temperature is constant (T_0). The top and bottom walls are parallel to the conducting board. In electronics cooling applications, the board covered with electronic components may face the smooth shields to avoid electro-magnetic interference from adjoining boards.

It is assumed that the flow is steady, incompressible, and laminar. In addition, the thermophysical proper-

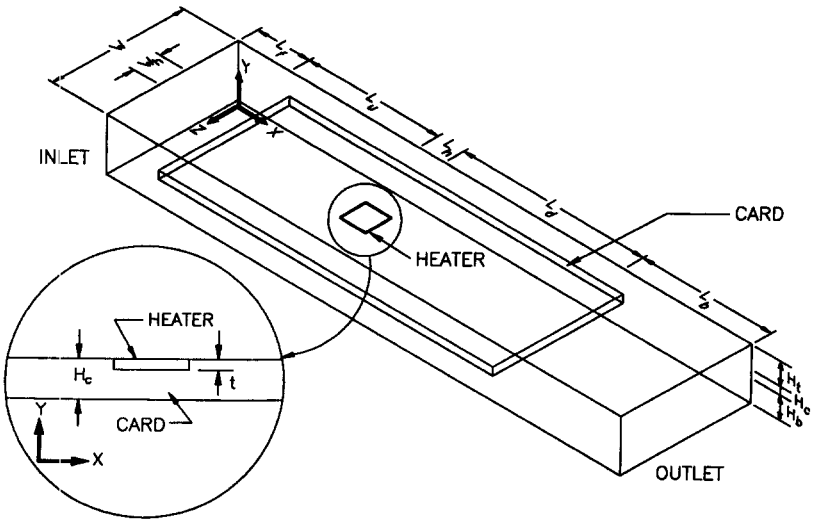

Fig. 1. (a) Schematic figure and coordinate diagram of the channel, (b) grid system.

ties are assumed to be constant. Based on the characteristic length H, the dimensionless variables are

$$X=\frac{x}{H} \quad Y=\frac{y}{H} \quad Z=\frac{z}{H} \tag{1a}$$

$$U=\frac{u}{u_0} \quad V=\frac{v}{u_0} \quad W=\frac{w}{u_0} \tag{1b}$$

$$\theta=\frac{T-T_0}{q'''H^2/k_s} \quad P=\frac{p}{\rho u_0^2} \tag{1c}$$

where u_0, T_0 and k_s represent the inlet velocity, inlet temperature and conductivity of the board, respectively. The corresponding dimensionless conservation equations for mass, momentum and energy are, respectively,

$$\frac{\partial U}{\partial X}+\frac{\partial V}{\partial Y}+\frac{\partial W}{\partial Z}=0 \tag{2}$$

$$U\frac{\partial U}{\partial X}+V\frac{\partial U}{\partial Y}+W\frac{\partial U}{\partial Z}= -\frac{\partial P}{\partial X}+\frac{1}{Re}\left(\frac{\partial^2 U}{\partial X^2}+\frac{\partial^2 U}{\partial Y^2}+\frac{\partial^2 U}{\partial Z^2}\right) \tag{3}$$

$$U\frac{\partial V}{\partial X}+V\frac{\partial V}{\partial Y}+W\frac{\partial V}{\partial Z}= -\frac{\partial P}{\partial Y}+\frac{1}{Re}\left(\frac{\partial^2 V}{\partial X^2}+\frac{\partial^2 V}{\partial Y^2}+\frac{\partial^2 V}{\partial Z^2}\right)+\frac{\kappa\cdot Gr}{Re^2}\theta \tag{4}$$

$$U\frac{\partial W}{\partial X}+V\frac{\partial W}{\partial Y}+W\frac{\partial W}{\partial Z}= -\frac{\partial P}{\partial Z}+\frac{1}{Re}\left(\frac{\partial^2 W}{\partial X^2}+\frac{\partial^2 W}{\partial Y^2}+\frac{\partial^2 W}{\partial Z^2}\right) \tag{5}$$

$$U\frac{\partial \theta}{\partial X}+V\frac{\partial \theta}{\partial Y}+W\frac{\partial \theta}{\partial Z}=\frac{\kappa^*}{Re\cdot Pr}\times\left(\frac{\partial^2 \theta}{\partial X^2}+\frac{\partial^2 \theta}{\partial Y^2}+\frac{\partial^2 \theta}{\partial Z^2}\right)+\frac{S}{\kappa} \tag{6}$$

where $\kappa^*=\kappa$ in the solid region and $\kappa^*=1$ in the fluid region. In addition, κ indicates the conductivity ratio, k_s/k_f. The source term (S) in the energy equation becomes unity in the region of the volumetric heat source; otherwise, this term disappears ($S=0$). In the solid region, the velocities are zero in the energy equation so that only conduction takes place. The boundary conditions can be readily non-dimensionalized, and they are omitted for the sake of brevity.

A control-volume-based finite difference program [19] has been used to solve the system of elliptic partial differential equations for pressure, velocity and temperature. The solution resulting from the control volume formulation implies that the conservation of mass, momentum and energy is exactly satisfied over the entire domain, as well as over any group of control volumes. After a series of test runs, a non-uniform mesh ($53\times32\times30$) was chosen for all cases. Further refinement showed minimal effect on the final results (less than 2% variation for θ_{max}). In addition, the harmonic mean formulation suggested by Patankar [19] was used to handle abrupt variations in thermophysical properties, such as the thermal conductivity across the interface of two different media. This approach ensures the continuity of the convective and diffusive fluxes across the interface without requiring the use of an excessively fine grid. Underrelaxation has been used to ensure convergence. For forced convection, the downstream boundary conditions have a limited influence on the outcome because of the strong parabolic characters of the problem. Hence, it was possible to obtain accurate results for the physical domain using an extended computational domain in the stream-wise direction.

For a typical run, the total number of iterations of equations (2)–(6) required to reach the steady-state was about 500 for forced convection and about 5000 for mixed and natural convection on a Convex 240.

An overall energy balance was used as an additional check on the accuracy of the results of each run. The difference between the heat input and the convective energy gain from inlet and the overall loss to exit is less than 5% for all cases.

3. RESULTS AND DISCUSSION

The present investigation focuses on the heat transfer characteristics resulting from the local buoyancy as well as the conjugate effects due to the thermally conducting board. The increase in air temperature, the heat transfer coefficient and the maximum temperature in the heat source are of practical interest. Calculations have been performed for $Pr = 0.71$, $1 \leqslant \kappa \leqslant 100$, $Gr = 7.8789 \times 10^7$ and $0.126 \leqslant Re \leqslant 1260$, respectively. First, $\kappa = 10$ was chosen to depict typical flow patterns, temperature and heat flux contours on the board surface, and the local Nusselt numbers in Figs. 2–6. Then, the importance of the conductivity ratio was addressed. The values for the key dimensionless variables are carefully selected to cover natural to mixed to forced convection. They may also represent realistic situations in many engineering applications. As an exemplary case, let us consider a 2 cm high channel (i.e. $H = 2$ cm). The corresponding average heat flux from the heat source becomes approximately 0.125 $W \cdot cm^{-2}$ ($q''' = 5\ W \cdot m^{-3}$), while the external velocity ranges from 1×10^{-4} to 1 $m \cdot s^{-1}$. In addition, the conductivity of the board ranges from 0.0263 to 2.63 $W \cdot (m \cdot K)^{-1}$. These dimensional numbers are appropriate for the air cooling of an electronic component mounted on a printed circuit board.

The velocity vectors in the mid-plane of Z-direction (i.e. $Z = 1.25$) have been plotted in Fig. 2 at the representative Reynolds numbers for all convection modes to display the role of natural convection in modifying the external fluid flow. When $Re = 1260$ (Fig. 2a), forced convection dominates the fluid flow pattern and the heat transfer process. As Re decreases to 12.6, the buoyancy effect becomes pronounced, and the strong interaction between the external flow and the natural convection cell is observed above the heater as depicted in Fig. 2b. On the other hand, a relatively weak buoyancy effect is noted under the board where forced convection predominates. This trend clearly indicates that the recirculating cells generated by the bottom heating case are much stronger than those generated by top heating.

Above the conducting board, it is interesting to observe that one recirculating cell (left) is attached to the top of the channel, while another one (right) is located near the conducting board; i.e. the external flow initially follows and then suppresses the counterclockwise recirculation cell and ultimately suppresses the clockwise second cell. A similar phenomenon was also observed using two-dimensional calculations in a channel [8]. At $Re = 0.126$ (Fig. 2c), flow patterns above and below the board are nearly symmetric about the mid-plane ($X = 3.75$) of the heat source, and natural convection completely dominates in both regions.

The dimensionless air temperature on the XZ plane at $Y = 0.5996$ is shown in Fig. 3. As for the velocity profile, the temperature distribution is symmetric with respect to the spanwise centerline of the heat source at a low Reynolds number. As the Reynolds number increases, the isotherms stretch toward the downstream direction. Although the board is thermally conducting, the effect of the heat source on the isotherms is limited to the downstream side of the heat source because of the relatively low thermal conductivity of the board. It is observed that more thermal energy is transferred toward the upstream side as the conductivity of the board increases. The dimensionless temperature on the top and bottom surfaces of the board ($Y = 0.575$ and 0.425) for $Re = 1260$ and 0.126 are shown in Figs. 4 and 5, respectively. When the Reynolds number is high (Fig. 4), a streamwise parabolic effect is noticeable downstream from the heat source. In this case, it is narrow spanwise. On the other hand, when Re is small, the effect of the heat source does not extend downstream. It is rather more pronounced in the spanwise direction as shown in Fig. 5 due to the influence of the recirculating cell around the heat source.

Figure 6 shows the dimensionless heat flux on the top surface of the board. When forced convection dominates, the heat transfer rate reaches maximum value at the leading edge of the heat source and decreases monotonically near the trailing edge as shown in Fig. 6a. The effects of mixed convection become pronounced as the external velocity decreases (Fig. 6b, c), and a decrease in the heat flux is particularly apparent near the inner portion of the heater surface. In the natural convection mode, the contour of the heat transfer rate is axisymmetric (Fig. 6d). When the Reynolds number is smaller than 2.5 as shown in Fig. 6c, d, there is a local minimum point on the heater surface. It is worth mentioning that $d\theta/dY$ becomes negative behind the heat source when $Re = 1260$ as shown in Fig. 6a. This can be explained by the fact that the air temperature is higher than the board temperature in that region, and therefore heat is transferred from the air to the board. This phenomenon is not observed in natural convection.

4. MODIFIED FIVE PERCENT DEVIATION RULE

To understand convective heat transfer characteristics on the surface of the board, let us introduce the local Nusselt number and the average Nusselt number, respectively,

$$Nu = \frac{hH}{k_f} = -\frac{1}{\theta}\frac{\partial \theta}{\partial n}\bigg|_s \tag{7}$$

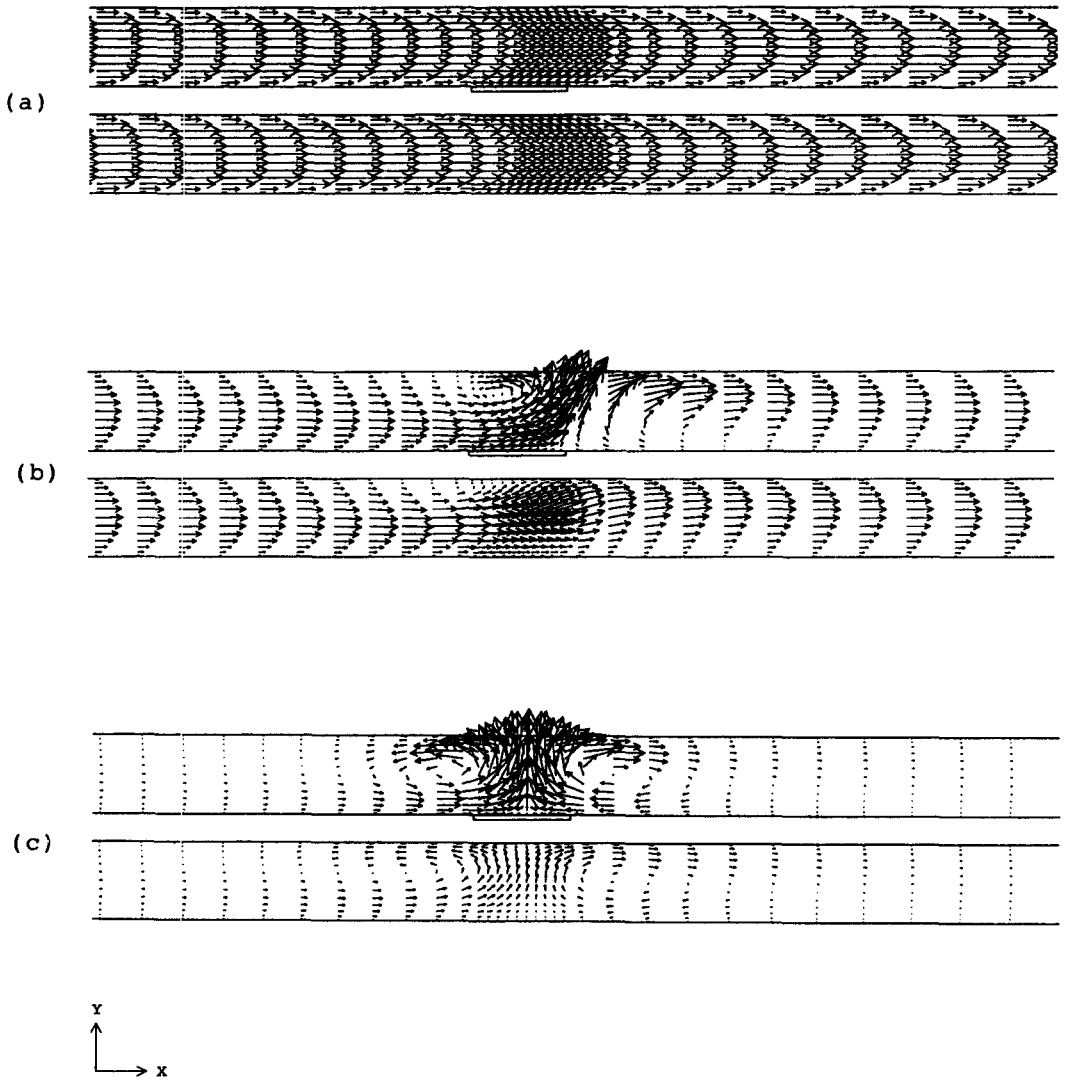

Fig. 2. Velocity vector field on XY-plane at $Z = 0.126$: (a) $Re = 1260$; (b) $Re = 12.6$; and (c) $Re = 0.126$.

and

$$\overline{Nu} = \frac{1}{A}\int_A Nu\,\mathrm{d}A \tag{8}$$

where n and the subscript 's' denote the normal direction from the wall and the surface of the board, respectively.

In Fig. 7, the calculated values (symbols) of the average Nusselt numbers on the top surface of the board are plotted as a function of $Re/Gr^{1/2}$ for different board conductivities. For small values of the abscissa, natural convection dominates, and therefore $\overline{Nu}$ corresponds to pure natural convection. For large values of the abscissa on the other hand, forced convection dominates. The well known '5% deviation rule' by Sparrow *et al.* [20] may be directly applied to the results. The rule states that a flow for which the average Nusselt number deviates by more than 5% from that for forced and natural convection is considered a mixed flow. The numerical heat transfer results can be reduced to a correlation between Nusselt, Grashof and Reynolds numbers. Correlation is sought in the form

$$\overline{Nu} = \left(C_1 + C_2 \cdot \frac{Re}{Gr^{1/2}}\right)^{C_3}. \tag{9}$$

Table 1 summarizes the constant values for three conductivity ratios, and the standard deviations are 0.395, 0.133 and 0.158 for $\kappa = 1$, 10 and 100, respectively. The corresponding regression lines are drawn in Fig. 7, and they fit well with the calculated values.

Further efforts have been made to simplify and improve the correlation including κ, which have resulted in a complex functional form with a relatively poor curve fitting to the calculated data set. In addition, the importance of either the local or the averaged Nusselt number on the heat source diminishes as κ increases due to the effects of thermal diffusion throughout the board. As an exemplary case,

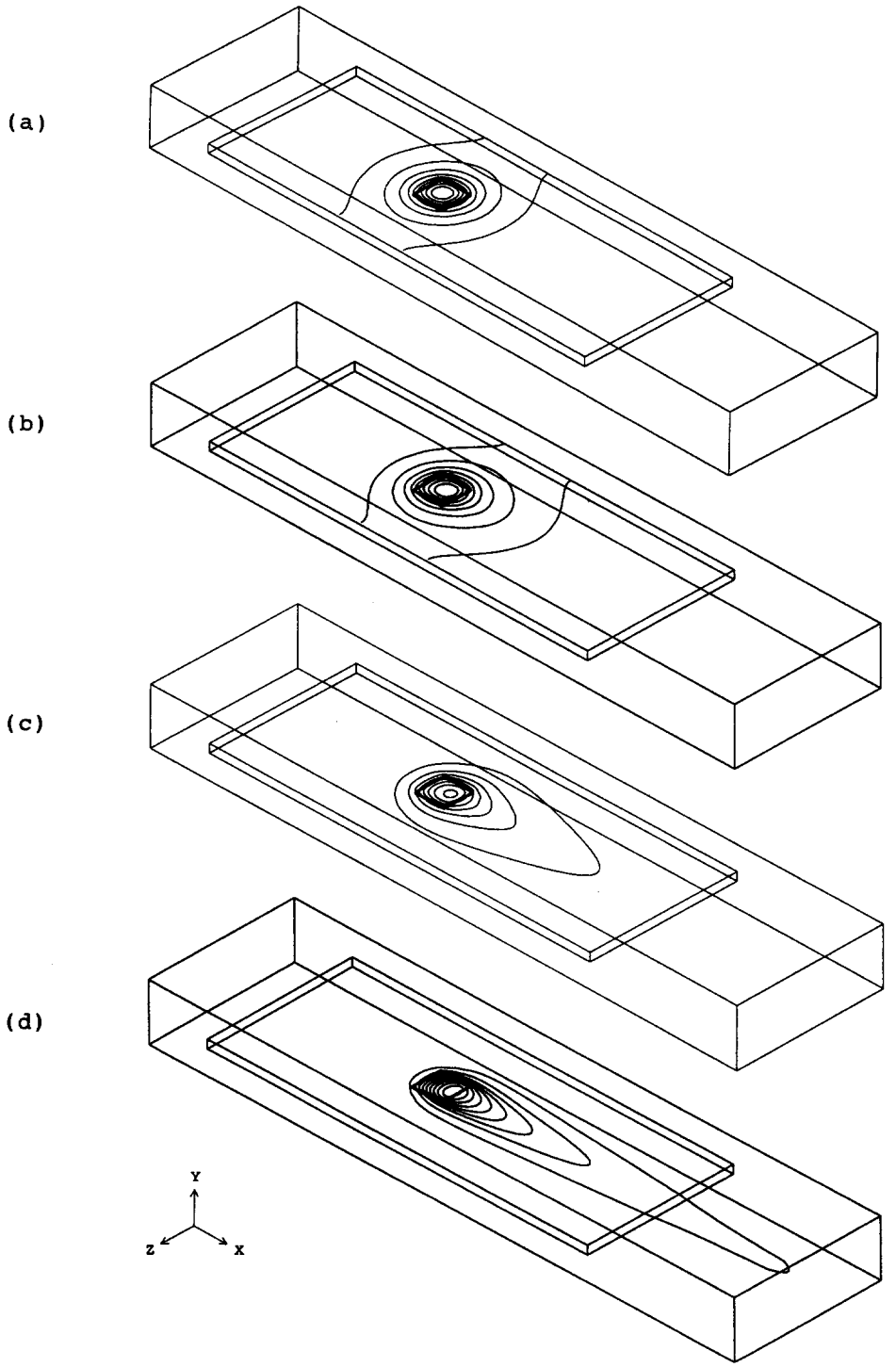

Fig. 3. Isotherms on XZ-plane at $Y = 0.5996$: (a) $Re = 0.126$; (b) $Re = 12.6$; (c) $Re = 126$; and (d) $Re = 1260$.

Fig. 8 shows the local Nusselt number on the top surface of the board at $Re = 639$ and $\kappa = 10$. Conjugate effects are pronounced near the heat source. In the upstream region of the heat source, thermal energy obviously transfers from the board to the approaching air. In the downstream region, however, the local Nusselt number becomes negative. This negative Nusselt number indicates that the thermal energy which convected from the top surface to the air in the upstream region is transferred back to the board. The energy is eventually transferred through the bottom surface of the board by convection. Obviously, the higher ther-

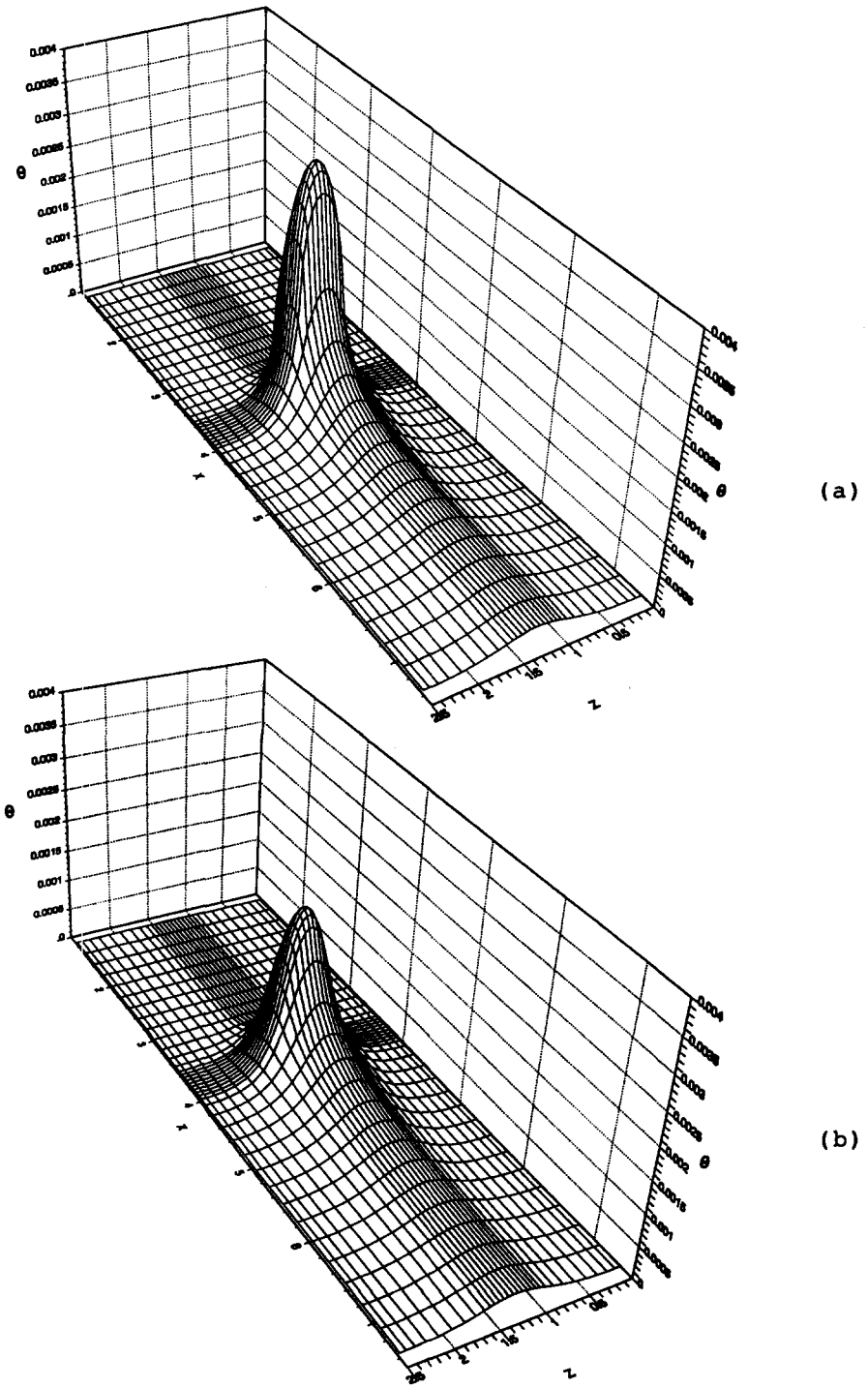

Fig. 4. Dimensionless temperature at $Re = 1260$: (a) top surface ($Y = 0.575$); (b) bottom surface ($Y = 0.425$).

mal conductivity of the board plays a crucial role in reducing Nu on the heat source and in increasing Nu adjacent to the heat source. Consequently, the area for which the average Nusselt number applies becomes nebulous, and therefore the usage of the average Nusselt number in conjunction with the '5% deviation rule' for conjugate heat transfer problems becomes questionable. This explains the poor curve fitting and the need for an alternative approach.

One of the most important objectives of thermal control in electronic packaging is to maintain the component temperature below the manufacturer's maximum specified operating temperature. For this reason, special attention is paid to the maximum tem-

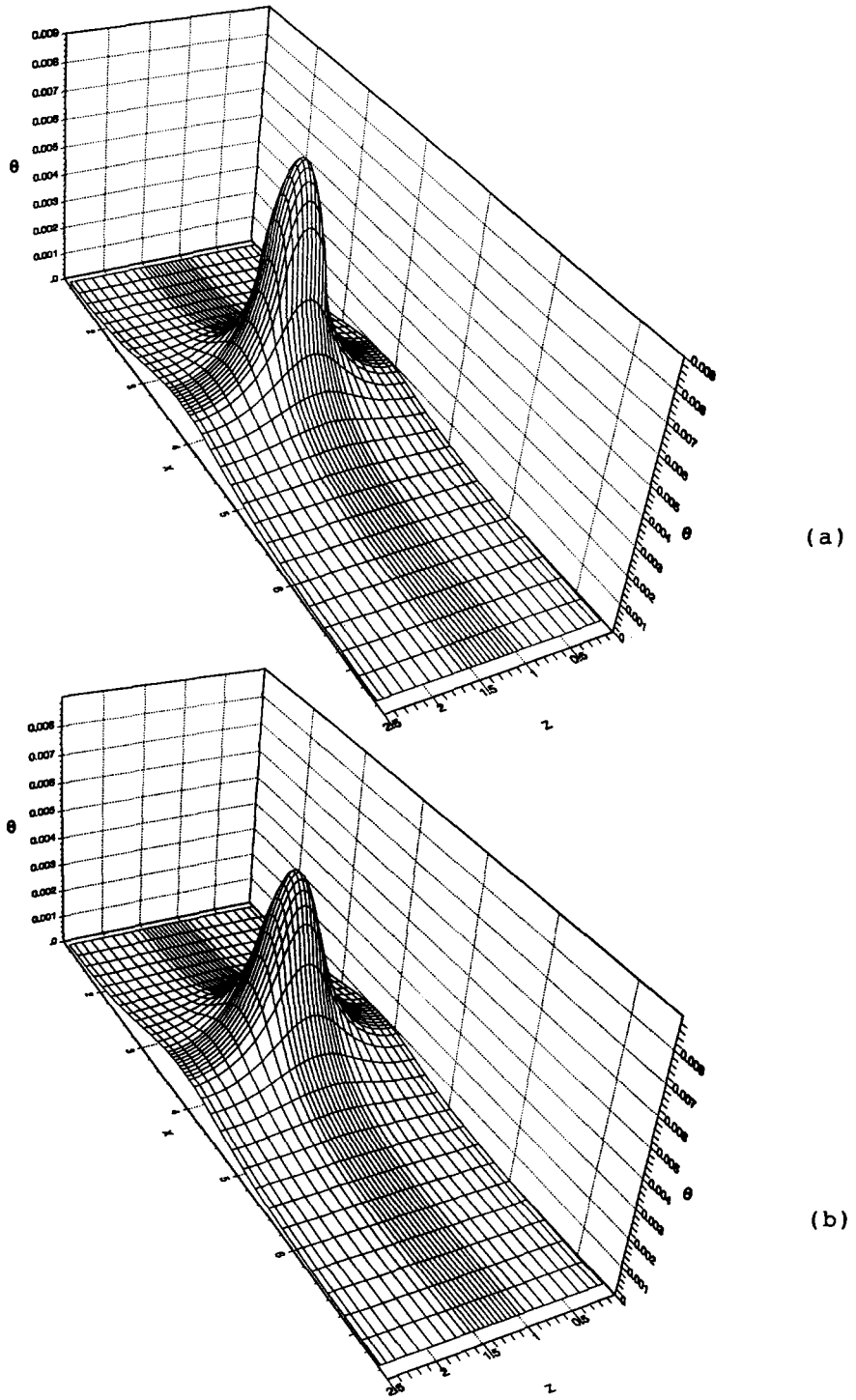

Fig. 5. Dimensionless temperature at $Re = 0.126$: (a) top surface ($Y = 0.575$); (b) bottom surface ($Y = 0.425$).

perature in the volumetric heat source (i.e. the overall maximum temperature in the present calculation domain), and calculations are repeated to obtain a correlation by replacing the average Nusselt number ($\overline{Nu}$) with the maximum dimensionless temperature (θ_{max}). The correlation including κ is

$$\theta_{max} = \kappa^{1/2}\left(C_4 + C_5 \cdot \frac{Re}{Gr^{1/2}}\right)^{-C_6} \tag{10}$$

where $C_4 = 8.39 \times 10^7$, $C_5 = 8.07 \times 10^9$ and $C_6 = -0.33$, respectively. The corresponding curve fit is much improved, in comparison with the previous attempt with $\overline{Nu}$; i.e. the difference between the numerical results and the values from the above correlation is generally less than 3%. At the extreme forced convection limit, however, there are a few exceptions due to the relatively small values of θ_{max} and the corresponding truncation errors. The curve fit is plotted in Fig. 9. Based on this correlation, the following criteria have been obtained in accordance with the '5% deviation rule'.

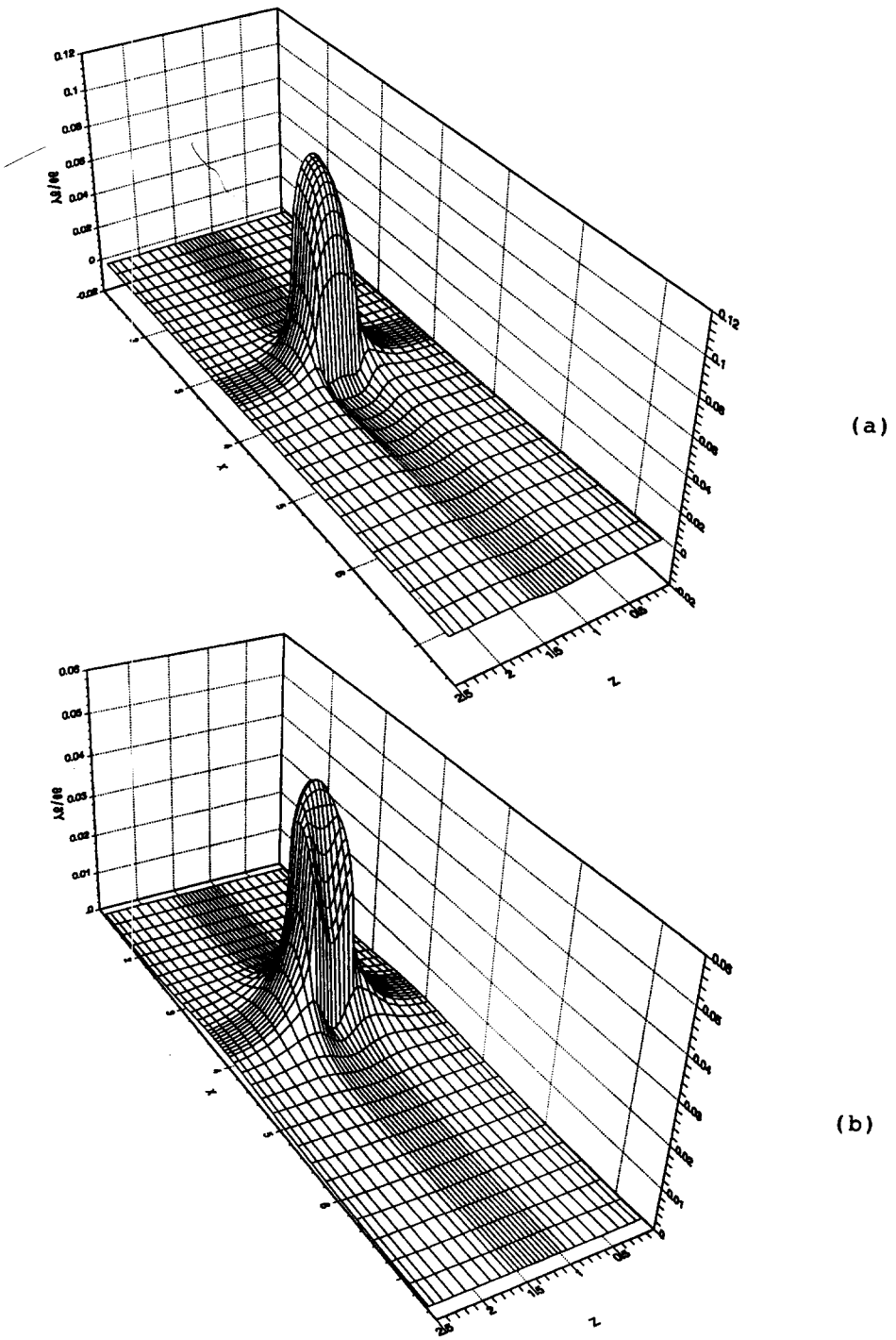

Fig. 6. Dimensionless heat flux on the top surface ($Y = 0.575$): (a) $Re = 1260$; (b) $Re = 12.6$; (c) $Re = 2.15$; and (d) $Re = 0.126$. (*Continued overleaf.*)

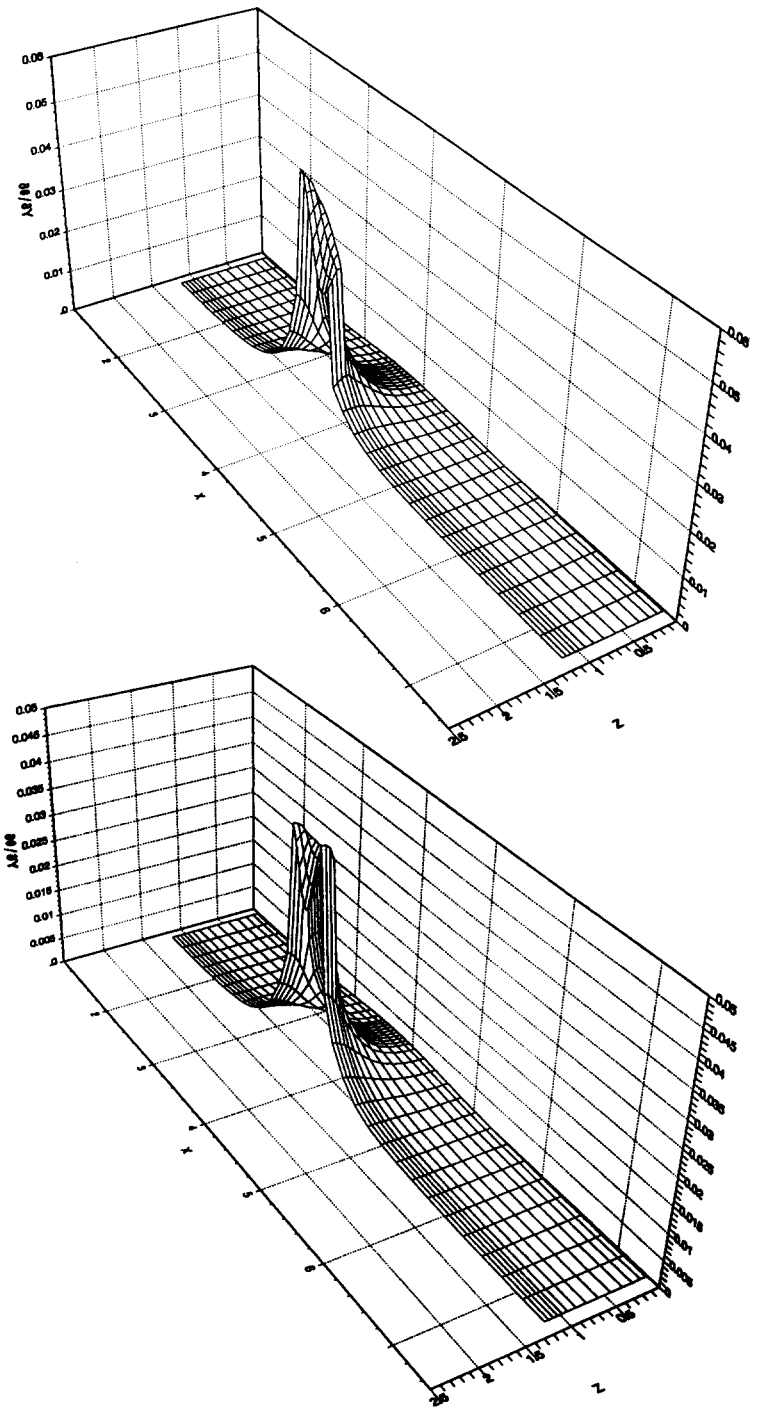

Fig. 6—*continued.*

(i) Natural convection regime

$$\frac{Re}{Gr^{1/2}} < 1.81 \times 10^{-3}.$$

(ii) Mixed convection regime

$$1.81 \times 10^{-3} \leqslant \frac{Re}{Gr^{1/2}} < 2.80 \times 10^{-2}.$$

(ii) Forced convection regime

$$\frac{Re}{Gr^{1/2}} \geqslant 2.80 \times 10^{-2}.$$

Each regime of convection is clearly defined and takes account of the influence of conduction throughout the board. Therefore, the present authors propose the 'modified 5% deviation rule.' This states that a

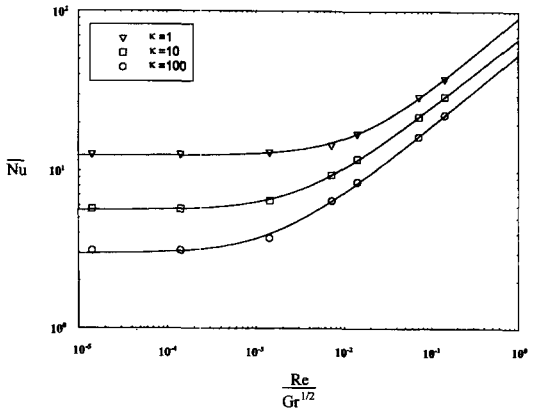

Fig. 7. Average Nusselt numbers on the top surface of the heat source vs Gr/Re^2.

Table 1. Coefficients for correlation (equation (9))

κ	C_1	C_2	C_3
1	225.95	16025.70	0.4655
10	55.15	19375.20	0.4297
100	11.29	7148.34	0.4493

flow for which a group of dimensionless variables differs by more than 5% from the asymptotes for natural and forced convection will be considered a mixed flow. Included among the dimensionless variables are the maximum dimensionless temperature and the conductivity ratio.

5. CONCLUSIONS

Three-dimensional mixed convection from a flush mounted heat source on a thermally conducting board has been numerically investigated. Emphasis has been placed on the interaction between the buoyancy-induced flow from an isolated heat source and the approaching external flow inside a rectangular channel. In the mixed convection regime, the local Nusselt number on the top surface of the heat source assumes a very different shape from that on the bottom surface. Three-dimensional effects are especially pronounced on the top surface. Recirculating cells, as well as streamwise and spanwise conduction throughout the board play a crucial role in determining heat transfer coefficients on the exposed surface. Correlations were

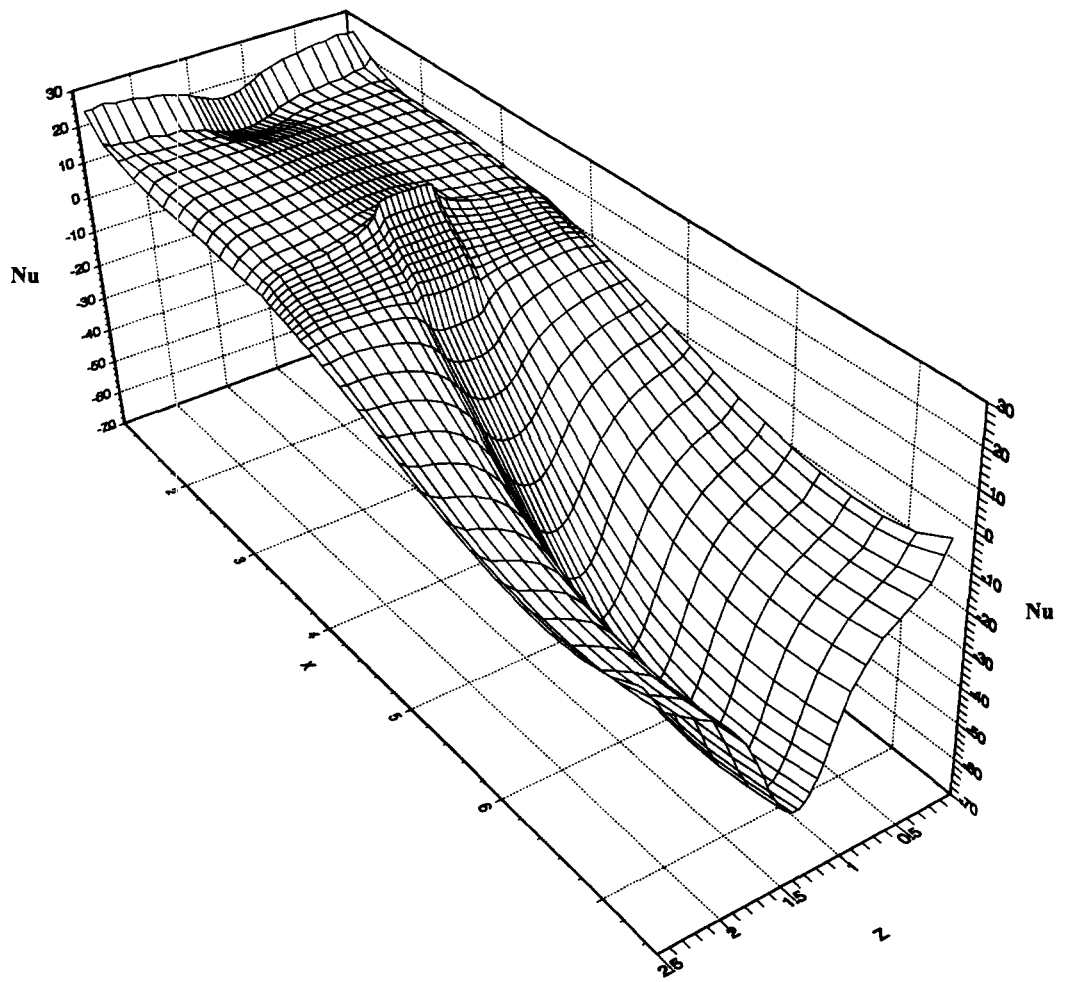

Fig. 8. Local Nusselt number on the surface of the board.

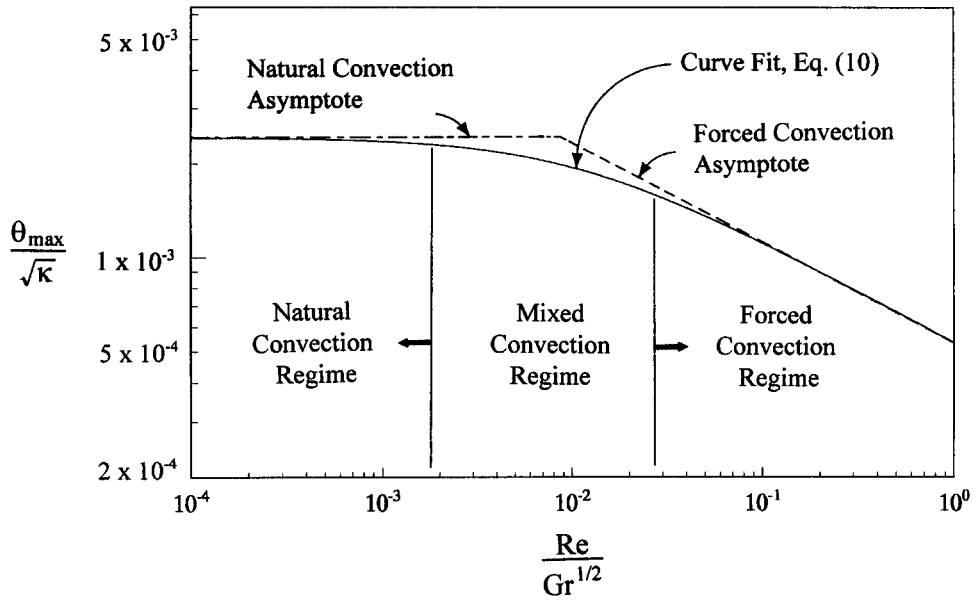

Fig. 9. Maximum dimensionless temperature vs Gr/Re^2.

obtained for the average Nusselt number as a function of the Grashof and Reynolds numbers. It was found that usage of the average Nusselt number was questionable in determining convection regimes for conjugate heat transfer problems. The 'modified 5% deviation rule' was proposed as an alternative to 'the 5% deviation rule.' The alternative rule uses the maximum dimensionless temperature as a function of the conductivity ratio, the Grashof number and the Reynolds number. The resultant correlation yields significantly better results than those obtained with the average Nusselt number.

REFERENCES

1. K. J. Kennedy and A. Zebib, Combined free and forced convection between horizontal parallel planes: some case studies, *Int. J. Heat Mass Transfer* **26,** 471–474 (1983).
2. J. Davalath and Y. Bayazitoglu, Forced convection cooling across rectangular blocks, *ASME J. Heat Transfer* **20,** 321–328 (1987).
3. E. Naito and Y. Nagano, Combined forced and free upward-flow convection in the entrance region between inclined parallel plates, *ASME J. Heat Transfer* **111,** 675–682 (1989).
4. A. Zebib and Y. K. Wo, A two-dimensional conjugate heat transfer model for forced air cooling of an electronic device, *ASME J. Electron. Packaging* **111,** 41–44 (1989).
5. D. Elpidorou, V. Prasad and V. Modi, Convection in a vertical channel with a finite wall heat source, *Int. J. Heat Mass Transfer* **34,** 573–578 (1991).
6. J. T. Lin, B. F. Armaly and T. S. Chen, Mixed convection heat transfer in inclined backward-facing step flows, *Int. J. Heat Mass Transfer* **34,** 1568–1571 (1991).
7. C. Yucel, M. Hasnaoui, L. Robillard and E. Bilgen, Mixed convection heat transfer in open ended inclined channels with discrete isothermal heating, *Numer. Heat Transfer*, Part A. **24,** 109–126 (1993).
8. C. Y. Choi and A. Ortega, Mixed convection in an inclined channel with a discrete heat source, *Int. J. Heat Mass Transfer* **36,** 3119–3134 (1993).
9. C. Y. Choi, S. J. Kim and A. Ortega, Effects of substrate and molding compound conductivity for convective cooling of electronic components, *ASME J. Electron. Packaging* **116,** 198–205 (1994).
10. S. Y. Kim, H. J. Sung and J. M. Hyun, Mixed convection from multiple-layered boards with cross streamwise periodic boundary conditions, *Int. J. Heat Mass Transfer* **35,** 2941–2952 (1992).
11. E. Papanicolaou and Y. Jaluria, Transition to a periodic regime in mixed convection in a square cavity, *J. Fluid Mech.* **239,** 489–509 (1992).
12. E. Papanicolaou and Y. Jaluria, Mixed convection from a localized heat source in a cavity with conducting walls: a numerical study, *Numer. Heat Transfer* Part A **23,** 463–484 (1993).
13. H. J. Shaw, W. L. Chen and C. K. Chen, Study on the laminar mixed convective heat transfer in three-dimensional channel with a thermal source, *ASME J. Electron. Packaging* **113,** 40–49 (1991).
14. H. V. Mahaney, S. Ramadhyani and F. P. Incropera, Numerical simulation of three-dimensional mixed convection heat transfer from an array of discrete heat sources in a horizontal rectangular duct, *Numer. Heat Transfer*, Part A **16,** 267–286 (1989).
15. J. R. Maughan and F. P. Incropera, Regions of heat transfer enhancement for laminar mixed convection in a parallel plate channel, *Int. J. Heat Mass Transfer* **33,** 555–570 (1990).
16. J. R. Maughan and F. P. Incropera, Use of vortex generators and ribs for heat transfer enhancement at the top surface of a uniformly heated horizontal channel with mixed convection flow, *ASME J. Heat Transfer* **113,** 504–507 (1991).
17. C. C. Huang and T. F. Lin, Buoyancy induced flow transition in mixed convective flow of air through a bottom heated horizontal rectangular duct, *Int. J. Heat Mass Transfer* **37,** 1235–1255 (1994).
18. K. C. Karki, P. S. Sathyamurthy and S. V. Patankar, Laminar mixed convection in a horizontal semicircular duct with axially nonuniform thermal boundary condition on the flat wall, *Numer. Heat Transfer* Part A **25,** 171–189 (1994).
19. S. V. Patankar, *Numerical Heat Transfer and Fluid Flow.* Hemisphere, New York (1980).
20. E. M. Sparrow, R. Eichhorn and J. L. Gregg, Combined forced and free convection in a boundary layer, *Phys. Fluids* **2,** 319–329 (1959).